DOI: 10.1002/chem.200902440

High Hole Mobility for a Side-Chain Liquid-Crystalline Smectic Polysiloxane Exhibiting a Nanosegregated Structure with a Terthiophene Moiety

Aya Matsui, Masahiro Funahashi,* Toru Tsuji, and Takashi Kato*[a]

Abstract: Side-chain liquid-crystalline siloxane polymers bearing terthiophene moieties as mesogenic pendant groups have been synthesized. An alkenylterthiophene derivative was treated with poly(hydrogenmethylsiloxane) and poly(dimethylsiloxane-*co*-hydrogenmethylsiloxane)s in Me_2SiO/MeHSiO ratios of 1:1 and 7:3, respectively, in the presence of the Karstedt catalyst, to produce pale yellow polymers. The degrees of introduction of the mesogenic unit were 100, 50, and 30%, respectively. The polymers exhibit ordered smectic phases at room temperature. The copolymers with dimethylsiloxane units form smectic phases as a consequence of nanosegregation between the mesogenic units and siloxane backbones with the alkylene spacers. Time-of-flight measurement reveals that the hole mobility exceeds $1\times10^{-2}\,cm^2V^{-1}s^{-1}$ in the ordered smectic phase of the copolymer with a degree introduction of the mesogenic units of 50%. This value is comparable to that of the highly ordered mesophases of low-molecular-weight derivatives of phenylnaphthalene and terthiophene. Because of the segregation behavior induced by the flexible backbone, a closer molecular packing structure favorable for fast carrier transport may be formed in the smectic phase of the copolymer in spite of the low density of the mesogenic groups.

Keywords: electron transport · liquid crystals · polymers · semiconductors · siloxanes

Introduction

For practical device fabrication, solution-processable organic semiconductors with sufficient mechanical strength and flexibility are useful.[1] For example, polymers with photoconductive pendant groups, such as polyvinylcarbazole, are solution-processable and have a sufficient mechanical strength and flexibility.[2] Thus, they have been utilized for xerographic photoreceptors[2a–f] and photorefractive devices.[3] However, their carrier mobilities are significantly low, of the order of 10^{-7}–$10^{-5}\,cm^2V^{-1}s^{-1}$, and depend significantly on the temperature and electric field.[2a–g] Their practical applications have been limited to optoelectronic devices that do not require a fast response speed and high operating current. This carrier transport characteristic originates from the large energetic and positional disorders as well as a small transfer integral between the pendant groups, due to their amorphous structure.[2b,f] The high density of the pendant groups and the small disorder should enhance carrier transport in the polymers. An improvement in hole transport was observed in isotactic poly(carbazolylethyl acrylate) when compared to the atactic counterparts, but the hole mobility did not exceed $10^{-4}\,cm^2V^{-1}s^{-1}$ at ambient temperature.[4]

The objective of this research was to synthesize side-chain liquid-crystalline polymeric semiconductors exhibiting high carrier mobilities. For this purpose, we designed side-chain liquid-crystalline polysiloxanes with π-conjugated groups. We expect these polymers to form nanosegregated structures that might enhance carrier transport.[5]

For low-molecular-weight liquid-crystalline molecules, electronic charge carrier transport has been observed[6] in the discotic columnar,[7,8] smectic,[9–11] and cholesteric phases.[12] Carrier transport in the liquid-crystalline phases is more efficient than in amorphous semiconductors. This is attributed to the reduced disorder and the increased transfer integral between the π-conjugated molecules in the liquid-crystalline structures.[6] However, a remarkable increase in carrier mobility has not been observed in side-chain liquid-crystalline polymers. For examples, the hole mobilities for nematic side-chain polymers that contain carbazole moieties were of the order of $10^{-7}\,cm^2V^{-1}s^{-1}$.[13a,b] Nematic side-chain

[a] A. Matsui, M. Funahashi, T. Tsuji, T. Kato
Department of Chemistry and Biotechnology
School of Engineering, The University of Tokyo
7-3-1 Hongo, Bunkyo-ku, Tokyo 113-8656 (Japan)
Fax: (+81) 3-5841-8661
E-mail: kato@chiral.t.u-tokyo.ac.jp
funahashi@chembio.t.u-tokyo.ac.jp

Supporting information for this article is available on the WWW under http://dx.doi.org/10.1002/chem.200902440.

polymers bearing oxadiazole moieties also exhibited low carrier mobilities of the order of $10^{-6}\,cm^2\,V^{-1}\,s^{-1}$.[13c] These values are comparable to those of amorphous polyvinylcarbazole derivatives.[2a–e] In general, higher carrier mobilities are observed in the smectic and columnar phases than in the nematic phase for low-molecular-weight liquid crystals.[12b] However, homogeneous thin films of smectic side-chain liquid-crystalline polymers with low defect density are not easily obtained, and thus low photoconductivity results.[14]

Herein we report hole transport in the nanosegregated structures of smectic liquid-crystalline side-chain siloxane copolymers. Terthiophene moieties as mesogenic pendant groups were attached to polysiloxane backbones containing flexible dimethylsiloxane segments, because high carrier mobilities were observed in the smectic phases of dialkylterthiophenes.[9c] Liquid-crystalline polysiloxane elastomers[15] and polysiloxane polymers bearing pendant triphenylene moieties that exhibit columnar mesophases have been synthesized, but their carrier transport has not been studied.[16]

Results and Discussion

Synthesis and characterization of polymers: Side-chain liquid-crystalline polymers **1a–c** were synthesized as shown in Scheme 1. The Suzuki coupling reaction between 2-(10-decenyl)thienyl-4,4,5,5-tetramethyl-1,3,2-dioxaborolane (**2**) and 5-bromo-5′-hexyl-2,2′-bithiophene (**3**) gave 5-(10-decenyl)-5″-hexyl-2,2′:5′,2″-terthiophene (**4**) with a double bond at the terminus of the alkyl side chain. Compound **4** was treated with poly(hydrogenmethylsiloxane) (**5a**, $M_n = 1400–1800$) and poly(dimethylsiloxane-*co*-hydrogenmethylsiloxane)s in Me_2SiO/MeHSiO ratios of 1:1 (**5b**: $M_n = 900–1200$) and 7:3 (**5c**: $M_n = 1900–2000$) in the presence of the (1,3-divinyl-1,1,3,3-tetramethyldisiloxane)platinum(0) complex (Karstedt catalyst)[17a,b] in toluene at 80 °C, to give siloxane polymers **1a–c**. When a conventional hydrosilylation catalyst, namely, hexachloroplatinic acid (Speier catalyst)[17c] was used, the mesogenic groups could not be introduced into the polysiloxane backbones.

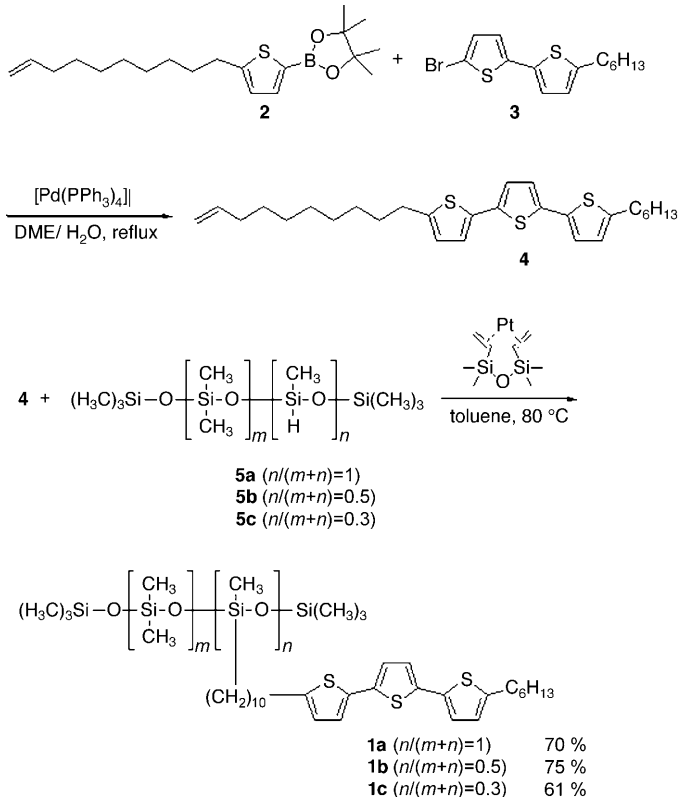

Scheme 1. Synthetic route to side-chain liquid-crystalline polymers **1a–c**.

The molecular structures of resulting polymers **1a–c** were characterized by means of ^1H NMR spectroscopy, IR spectroscopy, and gel permeation chromatography (GPC). Almost all the SiH sites in the backbones of polymers **1a–c** were substituted by mesogenic pendant groups. The number average molecular weight (M_n), molecular weight dispersivity (M_w/M_n), and ratio of the dimethylsiloxane and mesogenic units are given in Table 1.

Table 1. Mesomorphic properties and molecular weights of polymers **1a–c**.

	M_n	M_w/M_n	$n/(n+m)$[a]	Phase transition temperature [°C] (transition enthalpy [$J\,g^{-1}$])
1a	1.2×10^4	2.7	1	Sm[b] 109 (18.7) SmA 133 (18.7) Iso[c]
1b	5.6×10^3	1.5	0.5	Sm 95 (12.8) SmA 114 (25.7) Iso
1c	7.4×10^3	2.0	0.3	Sm 42 (3.12) SmB 89 (15.7) SmA 100 (10.8) Iso

[a] *m* and *n* are the average number of dimethylsiloxane units and siloxane moieties bearing a mesogenic group, respectively, as shown in Scheme 1. [b] Ordered smectic phase. [c] Isotropic phase.

Mesomorphic behavior of the polymers: The phase-transition behavior of polymers **1a–c** are summarized in Table 1. Copolymer **1b** exhibits two smectic phases and does not crystallize even below ambient temperature. In the differential scanning calorimetry (DSC) thermograms, two broad peaks are observed at 114 and 95 °C on cooling and at 97 and 117 °C on heating (Figure 1). No clear glass transitions

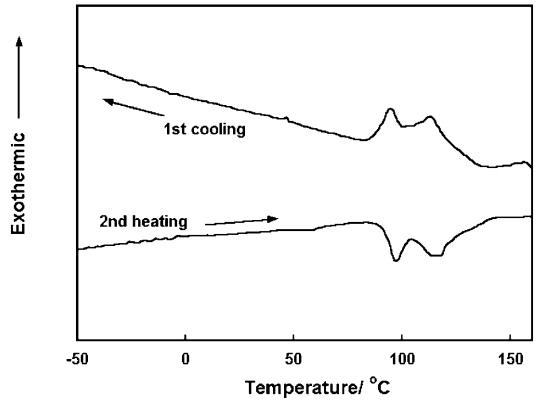

Figure 1. DSC thermograms of copolymer **1b**. The heating and cooling rates were 5 °C min^{-1}.

are observed above −80 °C. In the mesomorphic temperature region, fanlike textures, which are characteristic of smectic phases, are seen under a polarizing microscope (Figure 2). The domain size reaches several tens of micrometers.

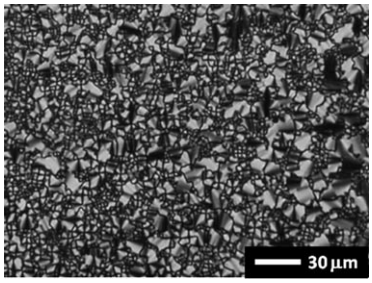

Figure 2. Photomicrograph of copolymer **1b** in the ordered smectic phase at RT under a polarizing microscope.

The liquid-crystalline structures of **1a–c** were examined by XRD (Figure 3). For **1b**, the XRD pattern reveals that the mesophases of copolymer **1b** are a smectic A (SmA) phase and an ordered smectic phase with a rectangular lattice. In the smectic A phase at 110 °C, one peak at 38 Å, corresponding to the layer spacing, is observed in the XRD profile. In the ordered smectic phase, the diffraction pattern shows a low-angle peak at 38 Å accompanied by higher-order diffraction peaks and three wide-angle peaks at 3.3, 4.0, and 4.6 Å (Figure 3b). The low-angle peak and related diffractions can be attributed to formation of a layer structure in the smectic phase. The peaks in the wide-angle region indicate a long-range rectangular order of the molecular position within the smectic layers. The diffraction pattern is similar to those in the E phase reported for low-molecular-weight liquid crystals.[18] The diffraction peaks of **1b** in the ordered smectic phase are broader than those in the ordered smectic phases of low-molecular-weight liquid crystals.[9e] The peaks at 3.3, 4.0, and 4.6 Å are assigned to the (021), (011), and (020) diffractions, respectively, and indicate the existence of the rectangular lattice in the mesophase.[18,19] The detailed assignment is given in the Supporting Information. In these phases, the layer spacing determined by diffraction in the low-angle region is larger than the length of the mesogenic unit with an all-*trans* conformation (32.5 Å), which was determined by molecular mechanics calculation (MM2 force field). This observation suggests that formation of a nanosegregated structure is enhanced by the sublayers consisting of dimethylsiloxane segments[5g,h] in polymer **1b**, which has a relatively high content of dimethylsiloxane units. The formation of the nanostructure and the sublayers is promoted by π–π interaction between the terthiophene moieties and the resulting segregation of the dimethylsiloxane units. Schematic illustrations of the nanosegregation of polymers **1a–c** are shown in Figure 4. Figure 4b shows the formation of the nanostructure and the sublayers for polymer **1b**.

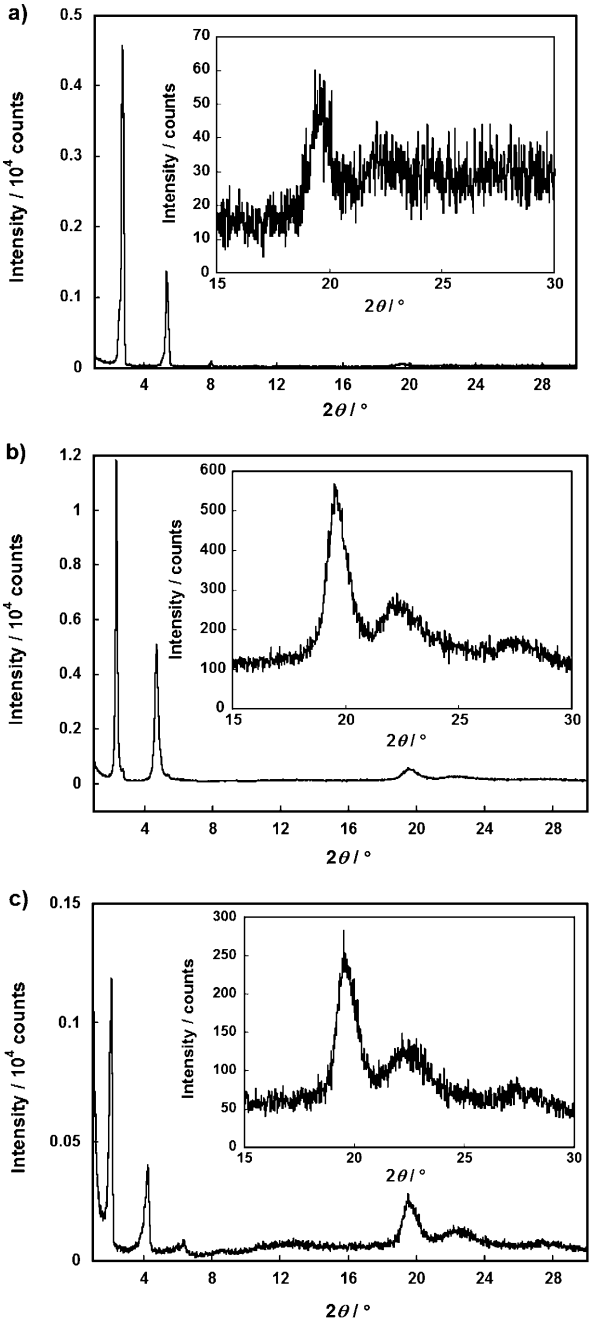

Figure 3. XRD patterns of the ordered smectic phase of a) polymer **1a**, b) copolymer **1b**, and c) copolymer **1c** at 30 °C. The insets are enlargements of the wide-angle region.

In the texture photomicrograph (Figure 2), relatively large domains with sizes of tens of micrometers are seen and defect lines characteristic of the ordered smectic phase are not observed. The distortion resulting from the phase transition from the SmA to the ordered smectic phase should be released, due to the flexibility of the polymer backbone.

Polymer **1a** also exhibits an SmA phase between 133 and 109 °C and an ordered smectic phase below 109 °C on cooling (see the Supporting Information). In the ordered smectic

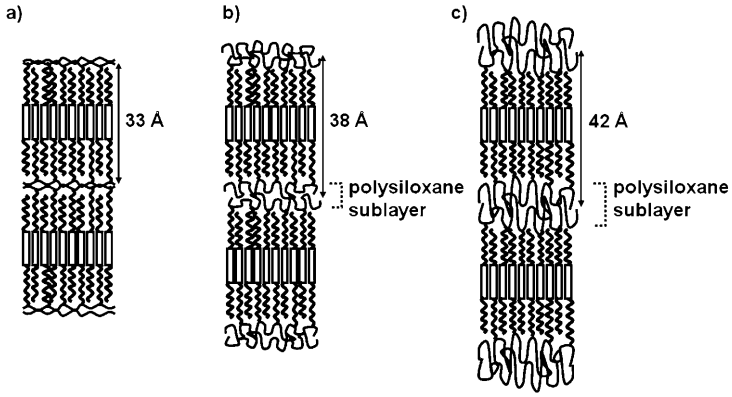

Figure 4. Schematic illustration of possible structures of the smectic polysiloxanes a) **1a**, b) **1b**, and c) **1c**.

phase, the diffraction pattern reveals a low-angle peak at 33 Å accompanied by higher-order diffraction peaks and one peak at 4.6 Å as well as an ambiguous broad peak around 4 Å in the wide-angle region. The polarizing photomicrograph shows a fanlike texture with defect lines, characteristic of the ordered smectic phase (see the Supporting Information), and the wide-angle peaks should be broadened by the large disorder of the smectic phase. The smectic layer spacing determined from the low-angle peak is almost identical to the length of the mesogenic side chain. No nanosegregated structure is observed for polymer **1a**.

For copolymer **1c**, the SmA phase is observed between 100 and 89 °C, the smectic B hexatic (SmB) phase between 89 and 42 °C, and the ordered smectic phase below 42 °C on cooling (see the Supporting Information). In the ordered smectic phase, the XRD pattern (Figure 3c) reveals a low-angle peak at 42 Å accompanied by higher order diffraction peaks and three peaks at 4.5, 3.9, 3.3 Å in the wide-angle region. The smectic layer spacing of 42 Å is greater than the length of the mesogenic side chain. This result also shows nanosegregation of mesogenic moieties from the dimethylsiloxane segments, as shown in Figure 4c. The intensities of the low-angle peaks are smaller than those in polymers **1a** and **1b**. These weak diffractions suggest that the layer structure should be more disordered than those of polymers **1a** and **1b**. The effects of the presence of the flexible dimethylsiloxane segments are more pronounced for copolymer **1c** than for **1b**. Unlike the nanosegregated structures of **1c**, a more highly interdigitated structure is also possible in the ordered smectic phases of polymers **1b** and **1c**. However, π–π interactions cannot promote formation of the rectangular lattice in the interdigitated structure, and the possible existence of the interdigitated structure should be ruled out.

Carrier transport of the polymers: The carrier transport characteristics of the synthesized polymers were examined by the conventional time-of-flight (TOF) technique.[20] A polymer sample was melted on a indium tin oxide (ITO)-coated glass plate and the resulting polymer droplet was pressed with another ITO-coated glass plate. After cooling to room temperature, it was fixed with glue. The thickness of the polymer sample was determined by interference fringes in the transmittance spectrum. The sample was mounted on a hot stage. The transient photocurrent induced by laser illumination (third harmonic generation of an Nd:YAG laser, $\lambda = 356$ nm) during the application of a DC voltage was recorded by a digital oscilloscope.

No changes in the micrographic textures of polymers **1a–c** were observed when electric fields of the order of 10^5 V cm^{-1} were applied to the samples. The polarizing microscopy observations showed that the mesogenic units of the polymers in the samples were aligned parallel to the electrode surface. Thus, carrier transport within a smectic layer perpendicular to the electrode surface should be observed in the TOF measurements.

For copolymer **1b**, nondispersive transient photocurrent curves for the hole are observed in the ordered smectic phase below 90 °C. Figure 5a shows the transient photocurrent curves for the hole at 27 °C. From the kink point in the linear plot of the transient photocurrent, the hole mobility was determined to be 1.0×10^{-2} cm^2 V^{-1} s^{-1} at 10^5 V cm^{-1}. The value is of the same order as those in the ordered smectic phase of monomeric phenylnaphthalene[9b] and alkynylterthiophene derivatives,[9e] and indicates that a long-range ordered structure is maintained in the smectic polymer film.

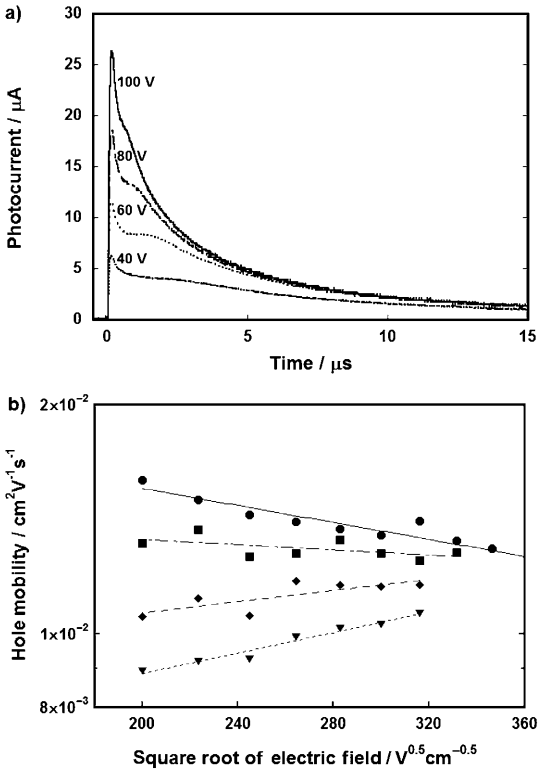

Figure 5. a) Transient photocurrent curves for the hole in the ordered smectic phase of side-chain liquid-crystalline polymer **1b** at 30 °C. The sample thickness was 10 μm. b) Hole mobility as a function of the square root of the electric field at 30 (▼), 45 (◆), 60 (■), and 80 °C (●).

This is the first example of a side-chain liquid-crystalline polymer with high carrier mobility exceeding $1\times10^{-2}\,cm^2V^{-1}s^{-1}$ at room temperature, determined by the TOF technique.

Figure 5b shows the hole mobility in the ordered smectic phase of copolymer **1b** as a function of the square root of the electric field at various temperatures. The hole mobility increases with increasing electric field and temperature below 60 °C. The dependence of the hole mobility on the electric field decreases with increasing temperature, and the dependence on the electric field becomes negative above 60 °C. This behavior is similar to that of amorphous organic semiconductors, such as photoconductive pendant polymers, which have disorders in the energy levels of hopping sites and the intermolecular distance.[2] The carrier transport characteristics also seem to be described by the Gaussian disorder model.[2f] The analysis based on the Gaussian disorder model reveals an energetic disorder of 53 meV, which is smaller than those of amorphous organic semiconductors. For the Gaussian disorder model, a temperature-independent structure is assumed. However, the molecular order is dependent on temperature for this polymer. In the XRD pattern of the ordered smectic phase, the wide-angle peaks associated with the molecular order within the smectic layers become sharper when the sample is cooled from 90 to 30 °C. These results show that the structure of the ordered smectic phase becomes more ordered with decreasing temperature. The temperature and field dependences of the hole mobility should be affected not only by the structural disorder, but also by the temperature dependence of the molecular ordering. To understand the detailed mechanism of carrier transport in the smectic phase of this copolymer, measurement of the hole mobility in a low-temperature region, in which the molecular order should be frozen, is necessary.

For polymer **1a**, dispersive transient photocurrent curves are observed in the ordered smectic phase for the hole. The hole mobility at room temperature was determined to be $4\times10^{-3}\,cm^2V^{-1}s^{-1}$ from the double-logarithmic plots of the transient photocurrents (see the Supporting Information). Above 50 °C, the transient photocurrent curves are fully dispersive. The transit times cannot be determined even from double-logarithmic plots. For polymer **1c**, only photocurrent decays are observed when the pulse laser illuminates the sample and no clear kink points appear in the photocurrent curves.

The hole mobility of copolymer **1b** is higher than that of polymer **1a**, despite the lower density of the terthiophene groups in **1b** compared to **1a**. The degree of introduction of the mesogenic units is only 50 % in copolymer **1b**. In organic amorphous semiconductors, the carrier mobility is strongly affected by the concentration of the hopping sites. The low concentration of the π-conjugated chromophores results in low carrier mobility.[2h] In the XRD pattern of the ordered smectic phase of copolymer **1b**, strong and clear peaks are observed in the wide-angle region, which indicates the closed packing structure of the mesogenic moieties. This structure is formed by nanosegregation of rigid terthiophene mesogenic pendant groups of flexible dimethylsiloxane segments. The holes are effectively transported between the mesogenic moieties. The polymer backbones including the dimethylsiloxane segments do not inhibit hole transport. The nanosegregated flexible dimethylsiloxane segments of copolymer **1b** should promote formation of the closed packing structure and improve the morphology of the polymer film as compared to polymer **1a** with no dimethylsiloxane segments.

The packing structure of the mesogenic terthiophene moieties within the smectic layers in the ordered smectic phase of polymer **1a** is more disordered than in copolymer **1b**. The wide-angle peaks are weak in the XRD pattern for the ordered smectic phase of polymer **1a**. This disordered structure is unfavorable for fast carrier transport. For the ordered smectic phase of copolymer **1c**, relatively weak diffraction peaks are obtained in the low-angle region in spite of clear diffraction peaks corresponding to molecular ordering within the smectic layers. These results suggest that the layer structure should be disordered because of the high density of flexible dimethylsiloxane segments. Coherent hole transport in the disordered mesomorphic structure should be difficult.

Comparison of the carrier transport properties: Side-chain liquid-crystalline copolymer **1b** exhibits high carrier mobilities of the order of $10^{-2}\,cm^2V^{-1}s^{-1}$. This value is four orders of magnitude higher than those of amorphous organic semiconductors including photoconductive pendant polymers and amorphous triphenylamine derivatives with low molecular weights.[2] The efficient hole transport of **1b** should be attributed to the closed molecular packing structure and the small disorder in the ordered smectic phase of this polymer.

The hole mobility of copolymer **1b** is comparable to those in the highly ordered smectic phases of low-molecular-weight liquid-crystalline semiconductors, such as alkynylterthiophene derivatives.[9c,e] The XRD pattern of copolymer **1b** indicates the presence of long-range molecular ordering within the smectic layers. However, the diffraction peaks are broad and the molecular arrangement is disordered compared to those in the smectic phases of the low-molecular-weight liquid crystals. The hole mobility of copolymer **1b** is very high in spite of the presence of dimethylsiloxane moieties that are not associated with the carrier transport process. One of the advantages of this liquid-crystalline polysiloxane over the low-molecular-weight liquid-crystalline semiconductors is the wide temperature range of the smectic phase in which high carrier mobilities are observed. The flexible polysiloxane backbones inhibit crystallization, which produces grain boundaries that degrade efficient carrier transport. Moreover, for copolymer **1b**, nanosegregation of the flexible backbones promotes self-assembly of the mesogenic pendant chromophores, resulting in a highly ordered structure and excellent carrier transport.

The number of liquid-crystalline semiconductors that exhibit high carrier mobilities in the mesophases at room tem-

perature is limited.[8c,9d,e,10a–c] It is significant that high carrier mobilities at room temperature are realized in a polymer system with good flexibility and mechanical strength. This high carrier mobility and flexibility of copolymer **1b** should be favorable for application in electronic papers and photorefractive materials.

Among polymeric liquid-crystalline semiconductors, polarized light emission and carrier transport of photopolymerized nematic thin films of fluorene derivatives were investigated.[21] The hole mobilities of the nematic polymer thin films were of the order of $10^{-5}\,cm^2V^{-1}s^{-1}$.[22] High hole mobilities up to $0.01\,cm^2V^{-1}s^{-1}$ were reported for the smectic phases of photopolymerized liquid-crystalline semiconductors.[23] However, there have been no reports regarding carrier transport characterized by the TOF technique in side-chain liquid-crystalline polymers which yield homogeneous thin films.

Conjugated polymers, such as poly(3-alkylthiophene) and poly(thienothiophene) derivatives, have been used in field-effect transistors (FETs),[24] and a few polymers exhibit high carrier mobilities exceeding $0.1\,cm^2V^{-1}s^{-1}$,[24c] which is comparable to those in devices based on molecular crystals. However, these high carrier mobilities are limited to two-dimensional thin interface areas between the dielectric and active layers of FET devices. In the bulk state, the carrier mobility is $10^{-3}\,cm^2V^{-1}s^{-1}$.[25] Liquid-crystalline poly(9,9-dialkylfluorene) derivatives exhibit high hole mobilities of the order of $10^{-3}\,cm^2V^{-1}s^{-1}$ in the bulk state, which were determined by the TOF method.[26] Polymer systems which exhibit high carrier mobilities exceeding $10^{-2}\,cm^2V^{-1}s^{-1}$ in the bulk state have been quite limited so far. For applications in solar cells and photorefractive materials, coherent carrier transport in the bulk states is very significant.

The molecular weights of the polymers obtained in this study are relatively low. Liquid crystals with an oligosiloxane moiety at the terminus of the alkyl chain and octasilsesquioxane bearing mesogenic groups were also synthesized.[27a–e] They exhibit smectic phases over wide temperature ranges. Crystalline oligomers bearing π-conjugated moieties were synthesized and their field-effect mobilities in the crystalline state examined.[27f] However, their characteristics strongly depend on the conditions of device fabrication. The maximum hole mobility of the device is of the order of $10^{-2}\,cm^2V^{-1}s^{-1}$. Therefore, it is notable that polymer **1b** shows carrier mobilities of the order of $10^{-2}\,cm^2V^{-1}s^{-1}$.

Conclusion

Side-chain liquid-crystalline polysiloxanes with terthiophene moieties as pendant groups and copolymers consisting of dimethylsiloxane and methylsiloxane units bearing mesogenic pendant groups have been synthesized. The polymers exhibit ordered smectic phases at room temperature. The copolymer in which terthiophene groups are attached to 50% of the siloxane units forms a nanostructured smectic phase by segregation of the mesogenic units and dimethylsiloxane backbone. The hole mobility of the copolymer determined by the TOF technique is $1\times10^{-2}\,cm^2V^{-1}s^{-1}$ at room temperature. This value is comparable to those in the highly ordered smectic phases of low-molecular-weight derivatives of phenylnaphthalene and terthiophene.

Experimental Section

All ^1H NMR and ^{13}C NMR spectra were recorded by using a JEOL JNM-LA400 spectrometer. FTIR measurements were conducted by using a Jasco FT/IR-660 Plus spectrometer. 5-Bromo-5′-hexyl-2,2′-bithiophene (**3**) was synthesized by using a literature procedure.[28] Polymers **5a–c** were purchased from Sigma–Aldrich and Gelest. A polarizing optical microscope Olympus DP70 equipped with a Mettler FP82HT hot stage was used for visual observation of optical textures. Differential scanning calorimetry (DSC) was conducted by using a Netzsch DSC 204 Phoenix instrument. X-ray diffraction (XRD) measurements were carried out by using a Rigaku RINT 2500 diffractometer with a heating stage and Ni-filtered $Cu_{K\alpha}$ radiation. Polymer molecular weight and dispersivity were determined by gel permeation chromatography (Japan Analytical Industry, LC-908) with polystyrene as a standard.

2-(10-Decenyl)thiophene: Thiophene (5.8 g, 69 mmol) was dissolved in THF (70 mL) and the solution stirred at 0°C. A solution of butyllithium in hexane (1.6 M, 34 mL, 55 mmol) was added dropwise to the solution. After stirring for 1.5 h, 1-bromo-10-decene (10 g, 46 mmol) was added. After stirring at RT for 15 h, the reaction mixture was heated to reflux for 1 h. Dilute hydrochloric acid was added to the reaction mixture with stirring. The organic layer was separated and the water phase was extracted with *n*-hexane. The combined organic phase was washed with brine and dried with magnesium sulfate. After evaporation of the volatile organic solvent, the residual oil was purified by column chromatography to give a colorless oil (9.8 g, 44 mmol, 96% yield). ^1H NMR (400 MHz, $CDCl_3$): $\delta=7.10$ (d, $J=4.4$ Hz, 1H), 6.91 (dd, $J=3.8$, 5.0 Hz, 1H), 6.77 (d, $J=3.2$ Hz, 1H), 5.81 (ddt, $J=17.2$, 10.4, 6.8 Hz, 1H), 4.99 (dd, $J=1.6$, 17.2 Hz, 1H) , 4.93 (dd, $J=1.0$, 10.2 Hz, 1H), 2.81 (t, $J=7.6$ Hz, 2H), 2.06 (dt, $J=7.2$, 7.0 Hz, 2H), 1.70–1.29 ppm (m, 12H); ^{13}C NMR (100 MHz, $CDCl_3$): $\delta=28.9$, 29.1, 29.3, 29.4, 29.9, 31.8, 33.8, 114.1, 122.7, 123.8, 126.6, 139.2, 145.8 ppm; IR (KBr disk): $\tilde{\nu}=909$, 992, 1439, 1460, 1640, 2853, 2926 cm^{-1}; elemental analysis calcd (%) for $C_{14}H_{22}S$: C 75.61, H 9.97; found: C 75.44, H 9.93.

2-(10-Decenyl)thienyl-4,4,5,5-tetramethyl-1,3,2-dioxaborolane (2): 2-(10-Decenyl)-thiophene (9.8 g, 44 mmol) was dissolved in THF (60 mL) and the solution cooled to 0°C. A solution of butyllithium in hexane (1.6 M, 36 mL, 57 mmol) was added dropwise. After stirring for 1 h, the reaction mixture was cooled to −78°C and a THF solution (6.0 mL) of 2-isopropoxy-4,4,5,5-tetramethyl-1,3,2-dioxaborolane (9.8 g, 53 mmol) was added over 10 min. The reaction mixture was stirred at RT for 1 h. Water was added, and the organic phase separated. The water phase was extracted with ethyl acetate, which was combined with the separated organic phase. The solution was washed with brine and dried over sodium sulfate. After evaporation of the volatile organic solvent, the crude oil was purified by column chromatography to give a colorless oil (8.0 g, 23 mmol, 52% yield). ^1H NMR (400 MHz, $CDCl_3$): $\delta=7.47$ (d, $J=3.2$ Hz, 1H), 6.85 (d, $J=3.6$ Hz, 1H), 5.81 (ddt,, $J=17.0$, 10.2, 6.8 Hz, 1H), 4.99 (dd, $J=1.8$, 17.0 Hz, 1H) , 4.9 (dd, $J=1.4$, 10.2 Hz, 1H), 2.85 (t, $J=7.6$ Hz, 2H), 2.03 (dt, $J=6.8$, 6.9 Hz, 2H), 1.70–1.27 ppm (m, 24H); ^{13}C NMR (100 MHz, $CDCl_3$): $\delta=24.7$, 28.9, 29.0, 29.1, 29.3, 29.3, 30.1, 31.7, 33.8, 83.9, 114.1, 125.8, 137.3, 139.2, 153.7 ppm; IR (KBr disk): $\tilde{\nu}=3076$, 2979, 2927, 2854, 1779, 1692, 1641, 1538, 1470, 1359, 1271, 1213, 1145, 1112, 1061, 1011, 995, 957, 908, 855, 808, 779, 723, 687, 665, 578 cm^{-1}; elemental analysis calcd (%) for $C_{20}H_{33}BO_2S$: C 68.96, H 9.55; found: C 68.77, H 9.47.

5-(10-Decenyl)-5″-hexyl-2,2′:5′,2″-terthiophene (4): 2-Decenylthenylboric acid pinacol ester (**2**; 8.0 g, 23 mmol), 5-bromo-5′-hexyl-2,2′-bithiophene (**3**; 6.5 g, 20 mmol), and tetrakis(triphenylphosphine)palladium (340 mg, 0.28 mmol) were dissolved in dimethoxyethane (100 mL). An aqueous so-

lution of potassium carbonate (70 mL, 20 wt%) was added to the solution, which was heated to reflux for 1 h. The reaction mixture was cooled to RT and the resulting precipitate collected by filtration. The crude mixture was purified by silica-gel column chromatography and recrystallized from *n*-hexane to give a pale yellow precipitate (7.0 g, 76% yield). ^{1}H NMR (400 MHz, $CDCl_3$): δ=6.97 (s, 2H), 6.96 (d, J=3.6 Hz, 2H), 6.67 (d, J=2.8 Hz, 2H), 5.81 (ddt, J=17.0, 10.2, 6.9 Hz, 1H) , 4.99 (dd, J=1.8, 17.0 Hz, 1H) , 4.93 (dd, J=2.6, 10.2 Hz, 1H), 2.78 (t, J=7.6 Hz, 4H), 2.04 (dt, J=7.2, 7.1 Hz, 2H), 1.70–1.30 (m, 20H), 0.89 ppm (t, J=6.4 Hz, 3H); ^{13}C NMR (100 MHz, $CDCl_3$): δ=14.1, 22.6, 28.9, 29.0, 29.1, 29.3, 29.4, 30.2, 30.2, 31.6, 31.8, 114.1, 123.1, 123.4, 124.8, 134.6, 136.1, 136.1, 139.2, 145.3, 145.4 ppm; IR (KBr disk): $\tilde{\nu}$=2956, 2920, 2851, 1467, 1446, 1060, 908, 851, 791 cm^{-1}; elemental analysis calcd (%) for $C_{28}H_{38}S_3$: C 71.43, H 8.14; found: C 71.45, H 8.13.

Siloxane polymer 1a: Mesogenic compound **4** (0.40 g, 0.85 mmol) and poly(hydrogenmethylsiloxane) (**5a**; 43 mg, 0.71 mmol) were dissolved in toluene (8 mL). A solution of (1,3-divinyl-1,1,3,3-tetramethyldisiloxane)-platinum(0) (0.1 M, 8.5 μmol) in xylene (3.8 μL) was then added to the solution, which was stirred at 80°C for 2 d. The reaction solution was poured into methanol, and the resulting precipitate collected by filtration. Precipitation was repeated until the unconverted mesogenic compound was not detected. Side-chain liquid-crystalline polymer **1a** with molecular weight of 12000 was obtained (70% yield). ^{1}H NMR (400 MHz, $CDCl_3$): δ=6.88 (br, 4H), 6.59 (br, 2H), 2.72 (br, 4H), 1.63 (br, 4H), 1.46 (br, 2H), 1.30–1.26 (br, 22H), 0.87 (br, 3H), 0.51 (br, 2H), 0.15 (br, 0.6H), 0.08–0.05 ppm (br, 3H); ^{13}C NMR (100 MHz, $CDCl_3$): δ=14.0, 22.6, 28.8, 29.8, 29.6, 30.2, 30.2, 31.5, 31.6 31.6, 123.2,123.4, 124.7, 124.7, 134.7, 134.7, 134.7, 136.1, 136.2 ppm; IR (KBr disc): $\tilde{\nu}$=3065, 2956, 2922, 2851, 2156, 1523, 1466, 1443, 1258, 1087, 1018, 906, 853, 791 cm^{-1}; elemental analysis calcd (%) for $C_{29}H_{39}OS_3Si$: C, 65.60; H, 7.97; found: C, 63.50; H, 7.82.

Siloxane copolymer 1b: Mesogenic compound **4** (0.40 g, 0.85 mmol) and poly(dimethylsiloxane-*co*-hydrogenmethylsiloxane) (**5b**; Me_2SiO:MeHSiO=1:1, 90 mg, 0.71 mmol) were dissolved in toluene (8 mL). A solution of (1,3-divinyl-1,1,3,3-tetramethyldisiloxane)platinum(0) (0.1 M, 8.5 μmol) in xylene (3.8 μL) was added to the solution, which was stirred at 80°C for one week. The reaction solution was then poured into methanol and the resulting precipitate collected by filtration. Precipitation was repeated until the unconverted mesogenic compound was not detected. Side-chain liquid-crystalline polymer **1b** with a molecular weight of 5600 was obtained (75% yield). ^{1}H NMR (400 MHz, $CDCl_3$): δ=6.93 (br, 4H), 6.64 (br, 2H), 2.75 (br, 4H), 1.65 (br, 4H), 1.30–1.26 (br, 28H), 0.89 (br, 3H), 0.50 (br, 2H), 0.14–0.32 ppm (br, 11H); ^{13}C NMR (100 MHz, $CDCl_3$): δ=14.0, 22.6, 28.8, 29.5, 29.7, 31.5, 31.6, 31.6, 123.2, 123.5, 124.7, 124.7, 134.7, 134.7, 136.2, 136.3 ppm; IR (KBr disk): $\tilde{\nu}$=3066, 2960, 2920, 2852, 2153, 1521, 1466, 1446, 1259, 1093, 1024, 909, 850, 791 cm^{-1}; elemental analysis calcd (%) for $C_{31}H_{48}O_2S_3Si_2$: C 61.53, H 8.00; found: C 61.30, H 8.06.

Siloxane copolymer 1c: Mesogenic compound **4** (0.40 g, 0.85 mmol) and poly(dimethylsiloxane-*co*-hydrogenmethylsiloxane) (**5c**; Me_2SiO:MeHSiO=7:3, 180 mg, 0.71 mmol) were dissolved in toluene (8 mL). A solution of (1,3-divinyl-1,1,3,3-tetramethyldisiloxane)platinum(0) (0.1 M, 17 μmol) in xylene (3.8 μL) was added to the solution, which was stirred at 80°C for one week. The reaction solution was then poured into methanol, and the resulting precipitate collected by filtration. Precipitation was repeated until the unconverted mesogenic compound was not detected. Side-chain liquid-crystalline polymer **1c** with molecular weight of 7400 was obtained (61% yield). ^{1}H NMR (400 MHz, $CDCl_3$): δ=6.93 (br, 4H), 6.64 (br, 2H), 2.75 (br, 4H), 1.65 (br, 4H), 1.51 (br, 6.5H), 1.30–1.26 (br, 22H), 0.89 (br, 3H), 0.50 (br, 2H), 0.14 (br, 0.4H), 0.07–0.04 ppm (br, 17H); ^{13}C NMR (100 MHz, $CDCl_3$): δ=14.0, 17.6, 22.6, 23.0, 28.8, 29.2, 29.5, 29.7, 30.2, 31.5, 31.6, 31.6, 33.4, 123.2, 123.5, 124.7, 134.7, 136.2 ppm; IR (KBr disk): $\tilde{\nu}$=3065, 2959, 2923, 2852, 2150, 1523, 1467, 1448, 1260, 1099, 1021, 909, 850, 793 cm^{-1}; elemental analysis calcd (%) for $C_{31}H_{48}O_2S_3Si_2$: C 57.44, H 8.02; found: C 56.44, H 7.94.

Time-of-flight technique: The time-of-flight apparatus consisted of a pulsed laser (third harmonic generation of an Nd:YAG laser (Continuum Minilite II; wavelength, 356 nm; pulse duration, 1 ns)) for excitation, the sample on a hot stage, a serial resistor, and a digital oscilloscope (Tektronics 3344B). All measurements were carried out under atmospheric conditions. The polymer was pressed between two ITO-coated glass plates and fixed with epoxide glue. The thickness of the polymer film was determined by interference fringes in the transmittance spectrum. An electric field was applied to the polymer sample and the pulse laser illuminated one side of the cell. The absorption coefficient of the sample was sufficiently high and the excitation pulse was absorbed near the illuminated electrode, producing a sheet of photocarriers. The carrier sheet drifts across the bulk of the sample, inducing a displacement current through the serial resistor. When the charge carriers arrive at the counter electrode, the current decreases to zero. Therefore, the kink point in the transient photocurrent curve corresponds to the transit time t_T. By using Equation (1), the carrier mobility μ can be calculated from t_T, sample thickness d, and applied voltage V.

$$\mu = \frac{d^2}{Vt_T} \quad (1)$$

Acknowledgements

This study was partially supported by the Creative Scientific Research of "Invention of Conjugated Electronic Structures and Novel Functions" (no. 16GS0209), Global COE Grants to Young Researchers of the Global COE Program for Chemistry Innovation through Cooperation of Science and Engineering from the Ministry of Education, Culture, Sports, Science, and Technology, and a Grant-in-Aid for Scientific Research (A) (no. 19205017, T.K.) from the Japan Society for the Promotion of Science (JSPS).

[1] a) B. C. Thompson, J. M. J. Fréchet, *Angew. Chem.* **2008**, *120*, 62–82; *Angew. Chem. Int. Ed.* **2008**, *47*, 58–77; b) S. A. Jenekhe, *Nat. Mater.* **2008**, *7*, 354–355; c) A. Salleo, *Mater. Today* **2007**, *10*, 38–45; d) R. H. Friend, R. W. Gymer, A. B. Holmes, J. H. Burroughes, R. N. Marks, C. Taliani, D. D. C. Bradley, D. A. Dos Santos, J. L. Brédas, M. Lögdlund, W. R. Salaneck, *Nature* **1999**, *397*, 121–128; e) A. Dodabalapur, *Mater. Today* **2006**, *9*, 24–30; f) S. Allard, M. Forster, B. Souharce, H. Thiem, U. Scherf, *Angew. Chem.* **2008**, *120*, 4138–4167; *Angew. Chem. Int. Ed.* **2008**, *47*, 4070–4098.

[2] a) P. M. Borsenberger, D. S. Weiss, *Organic Photoreceptors for Xerography*, Marcel Dekker, New York, **1998**; b) M. van der Auweraer, F. C. De Schryver, P. M. Borsenberger, H. Bässler, *Adv. Mater.* **1994**, *6*, 199–213; c) M. Biswas, S. K. Das, *Polymer* **1982**, *23*, 1713–1726; d) J.-F. Morin, M. Leclerc, D. Adès, A. Siove, *Macromol. Rapid Commun.* **2005**, *26*, 761–778; e) J. V. Grazulevicius, P. Strohriegl, J. Pielichowski, K. Pielichowski, *Prog. Polym. Sci.* **2003**, *28*, 1297–1353; f) H. Bässler, *Phys. Status Solidi B* **1993**, *175*, 15–56; g) Y. Shirota, *J. Mater. Chem.* **2005**, *15*, 75–93; h) W. D. Gill, *J. Appl. Phys.* **1972**, *43*, 5033–5040; i) Y. Ohsedo, I. Imae, Y. Shirota, *Synth. Met.* **1999**, *102*, 969–970; j) Y. Ohsedo, I. Imae, Y. Shirota, *J. Polym. Sci. Part B: Polym. Phys.* **2003**, *41*, 2471–2484.

[3] a) P. Strohriegl, J. V. Grazulevicius, *Adv. Mater.* **2002**, *14*, 1439–1452; b) L. Paelke, H.-S. Kitzerow, P. Strohriegl, *Appl. Phys. Lett.* **2005**, *86*, 031104.

[4] a) T. Uryu, H. Ohkawa, R. Oshima, *Macromolecules* **1987**, *20*, 712–716; b) T. Uryu, H. Ohkawa, R. Oshima, *J. Polym. Sci. Part B: Polym. Phys.* **1988**, *26*, 1227–1236.

[5] a) T. Kato, *Science* **2002**, *295*, 2414–2418; b) C. Tschierske, *J. Mater. Chem.* **2001**, *11*, 2647–2671; c) T. Kato, N. Mizoshita, K. Kishimoto, *Angew. Chem.* **2006**, *118*, 44–74; *Angew. Chem. Int. Ed.* **2006**, *45*, 38–68; d) C. Tschierske, *Chem. Soc. Rev.* **2007**, *36*, 1930–1970; e) M. Prehm, C. Enders, M. Y. Anzahaee, B. Glettner, U. Baumeister, C. Tschierske, *Chem. Eur. J.* **2008**, *14*, 6352–6368; f) K. Kishimoto, M. Yoshio, T. Mukai, M. Yoshizawa, H. Ohno, T. Kato, *J. Am. Chem. Soc.* **2003**, *125*, 3196–3197; g) S. Diele, S. Oelsner, F. Kuschel, B. Hisgen, H. Ringsdorf, R. Zentel, *Makromol. Chem.* **1987**, *188*,

1993–2000; h) M. Rössle, L. Braun, D. Schollmeyer, R. Zentel, J. P. F. Lagerwall, F. Giesselmann, R. Stannarius, *Liq. Cryst.* **2005**, *32*, 533–538; i) L. Zhi, K. Müllen, *J. Mater. Chem.* **2008**, *18*, 1472–1484; j) T. Kato, T. Yasuda, Y. Kamikawa, M. Yoshio, *Chem. Commun.* **2009**, 729–739; k) K. Tanabe, T. Yasuda, T. Kato, *Chem. Lett.* **2008**, *37*, 1208–1209; l) A. Mishra, C.-Q. Ma, P. Bäuerle, *Chem. Rev.* **2009**, *109*, 1141–1276; m) N. Yoshimoto, J. Hanna, *Adv. Mater.* **2002**, *14*, 988–991; n) K. Isoda, T. Yasuda, T. Kato, *Chem. Asian J.* **2009**, *4*, 1619–1625; o) T. Kato, K. Tanabe, *Chem. Lett.* **2009**, *38*, 634–639.

[6] a) M. O'Neill, S. M. Kelly, *Adv. Mater.* **2003**, *15*, 1135–1146; b) Y. Shimizu, K. Oikawa, K. Nakayama, D. Guillon, *J. Mater. Chem.* **2007**, *17*, 4223–4229; c) M. Funahashi, H. Shimura, M. Yoshio, T. Kato, *Struct. Bonding (Berlin)* **2008**, *128*, 151–179; d) S. Sergeyev, W. Pisula, Y. H. Geerts, *Chem. Soc. Rev.* **2007**, *36*, 1902–1929; e) W. Pisula, M. Zorn, J. Y. Chang, K. Müllen, R. Zentel, *Macromol. Rapid Commun.* **2009**, *30*, 1179–1202; f) S. Laschat, A. Baro, N. Steinke, F. Giesselmann, C. Hägele, G. Scalia, R. Judele, E. Kapatsina, S. Sauer, A. Schreivogel, and M. Tosoni, *Angew. Chem.* **2007**, *119*, 4916–4973; *Angew. Chem. Int. Ed.* **2007**, *46*, 4832–4887; g) M. Funahashi, *Polym. J.* **2009**, *41*, 459–469.

[7] a) N. Boden, R. J. Bushby, J. Clements, M. V. Jesudason, P. F. Knowles, G. Williams, *Chem. Phys. Lett.* **1988**, *152*, 94–99; b) N. Boden, R. J. Bushby, J. Clements, B. Movaghar, K. J. Donovan, T. Kreouzis, *Phys. Rev. B*, **1995**, *52*, 13274–13280; c) D. Adam, F. Closs, T. Frey, D. Funhoff, D. Haarer, H. Ringsdorf, P. Schuhmacher, K. Siemensmeyer, *Phys. Rev. Lett.* **1993**, *70*, 457–460; d) D. Adam, P. Schuhmacher, J. Simmerer, L. Häußling, K. Siemensmeyer, K. Etzbach, H. Ringsdorf, D. Haarer, *Nature* **1994**, *371*, 141–143; e) T. Yasuda, H. Ooi, J. Morita, Y. Akama, K. Minoura, M. Funahashi, T. Shimomura, and T. Kato, *Adv. Funct. Mater.* **2009**, *19*, 411–419.

[8] a) A. M. van de Craats, J. M. Warman, K. Müllen, Y. Geerts, J. D. Brand, *Adv. Mater.* **1998**, *10*, 36–38; b) A. M. van de Craats, J. M. Warman, A. Fechtenkötter, J. D. Brand, M. A. Harbison, K. Müllen, *Adv. Mater.* **1999**, *11*, 1469–1472; c) W. Pisula, A. Menon, M. Stepputat, I. Lieberwirth, U. Kolb, A. Tracz, H. Sirringhaus, T. Pakula, K. Müllen, *Adv. Mater.* **2005**, *17*, 684–689.

[9] a) M. Funahashi, J. Hanna, *Appl. Phys. Lett.* **1997**, *71*, 602–604; b) M. Funahashi, J. Hanna, *Appl. Phys. Lett.* **1998**, *73*, 3733–3735; c) M. Funahashi, J. Hanna, *Appl. Phys. Lett.* **2000**, *76*, 2574–2576; d) M. Funahashi, J. Hanna, *Adv. Mater.* **2005**, *17*, 594–598; e) M. Funahashi, F. Zhang, N. Tamaoki, J. Hanna, *ChemPhysChem* **2008**, *9*, 1465–1473.

[10] a) M. Funahashi, F. Zhang, N. Tamaoki, *Adv. Mater.* **2007**, *19*, 353–358; b) F. Zhang, M. Funahashi, N. Tamaoki, *Appl. Phys. Lett.* **2007**, *91*, 063515; c) F. Zhang, M. Funahashi, N. Tamaoki, *Org. Electron.* **2009**, *10*, 73–84.

[11] K. Oikawa, H. Monobe, J. Takahashi, K. Tsuchiya, B. Heinrich, D. Guillon, Y. Shimizu, *Chem. Commun.* **2005**, 5337–5339.

[12] a) M. Funahashi, N. Tamaoki, *ChemPhysChem* **2006**, *7*, 1193–1197; b) M. Funahashi, N. Tamaoki, *Chem. Mater.* **2007**, *19*, 608–617; c) K. L. Woon, M. P. Aldred, P. Vlachos, G. H. Mehl, T. Stirner, S. M. Kelly, M. O'Neill, *Chem. Mater.* **2006**, *18*, 2311–2317; d) K. Tokunaga, Y. Takayashiki, H. Iino, J. Hanna, *Phys. Rev. B* **2009**, *79*, 033201.

[13] a) T. Ikeda, H. Mochizuki, Y. Hayashi, M. Sisido, T. Sasakawa, *J. Appl. Phys.* **1991**, *70*, 3689–3695; b) T. Ikeda, H. Mochizuki, Y. Hayashi, M. Sisido, T. Sasakawa, *J. Appl. Phys.* **1991**, *70*, 3696–3702; c) M. Kawamoto, H. Mochizuki, T. Ikeda, H. Iino, J. Hanna, *J. Phys. Chem. B* **2005**, *109*, 9226–9230; d) Y. Kosakasup, T. Kato, T. Uryu, *J. Polym. Sci., Part A: Polym. Chem.* **1994**, *32*, 711–719.

[14] M. Lux, P. Strohriegl, H. Höcker, *Makromol. Chem.* **1987**, *188*, 811–820.

[15] a) H. Finkelmann, G. Rehage, *Makromol. Chem. Rapid Commun.* **1980**, *1*, 31–34; b) J. Küpfer, H. Finkelmann, *Makromol. Chem. Rapid Commun.* **1991**, *12*, 717–726; c) E. Nishikawa, H. Finkelmann, *Macromol. Rapid Commun.* **1997**, *18*, 65–71; d) A. Komp, H. Finkelmann, *Macromol. Rapid Commun.* **2007**, *28*, 55–62.

[16] H. Bengs, H. Finkelmann, J. Küpfer, H. Ringsdorf, P. Schumacher, *Makromol. Chem. Rapid Commun.* **1993**, *14*, 445–450.

[17] a) B. D. Karstedt, US-A 3,775,452, **1973**; b) L. N. Lewis, R. E. Colborn, H. Grade, G. L. Bryant, Jr., C. A. Sumpter, R. A. Scott, *Organometallics* **1995**, *14*, 2202–2213; c) J. L. Speier, J. A. Webster, G. H. Barnes, *J. Am. Chem. Soc.* **1957**, *79*, 974–979.

[18] a) A. de Vries, *Mol. Cryst. Liq. Cryst.* **1985**, *131*, 125–145; b) S. Diele, D. Jaeckel, D. Demus, H. Sackmann, *Cryst. Res. Technol.* **1982**, *17*, 1591–1598.

[19] P. A. C. Gane, A. J. Leadbetter, *J. Phys. C* **1983**, *16*, 2059–2068.

[20] R. G. Kepler, *Phys. Rev.* **1960**, *119*, 1226–1229.

[21] K. L. Woon, M. O'Neill, G. J. Richards, M. P. Aldred, S. M. Kelly, A. M. Fox, *Adv. Mater.* **2003**, *15*, 1555–1558.

[22] S. R. Farrar, A. E. A. Contoret, M. O'Neill, J. E. Nicholls, G. J. Richards, S. M. Kelly, *Phys. Rev. B*, **2002**, *66*, 125107.

[23] R. J. Baldwin, T. Kreouzis, M. Shkunov, M. Heeney, W. Zhang, I. McCulloch, *J. Appl. Phys.* **2007**, *101*, 023713.

[24] a) Z. Bao, A. Dodabalapur, A. J. Lovinger, *Appl. Phys. Lett.* **1996**, *69*, 4108–4110; b) H. Sirringhaus, P. J. Brown, R. H. Friend, M. M. Nielsen, K. Bechgaard, B. M. W. Langeveld-Voss, A. J. H. Spiering, R. A. J. Janssen, E. W. Meijer, P. Herwig, D. M. de Leeuw, *Nature* **1999**, *401*, 685–688; c) I. McCulloch, M. Heeney, C. Bailey, K. Genevicius, I. MacDonald, M. Shkunov, D. Sparrowe, S. Tierney, R. Wagner, W. Zhang, M. L. Chabinyc, R. J. Kline, M. D. McGehee, M. F. Toney, *Nat. Mater.* **2006**, *5*, 328–333.

[25] S. S. Pandey, W. Takashima, S. Nagamatsu, T. Endo, M. Rikukawa, K. Kaneto, *Jpn. J. Appl. Phys., Part 2* **2000**, *39*, L94–L97.

[26] a) M. Redecker, D. D. C. Bradley, M. Inbasekaran, E. P. Woo, *Appl. Phys. Lett.* **1999**, *74*, 1400–1402; b) G. Heliotis, S. A. Choulis, G. Itskos, R. Xia, R. Murray, P. N. Stavrinou, D. D. C. Bradley, *Appl. Phys. Lett.* **2006**, *88*, 081104.

[27] a) I. M. Saez, J. W. Goodby, *Structure and Bonding*, **2008**, *128*, 1–62; b) G. H. Mehl, J. W. Goodby, *Chem. Ber.* **1996**, *129*, 521–525; c) D. J. Gardiner, H. J. Coles, *J. Appl. Phys.* **2006**, *100*, 124903; d) G. H. Mehl, J. W. Goodby, *Angew. Chem.* **1996**, *108*, 2791–2793; *Angew. Chem. Int. Ed. Engl.* **1996**, *35*, 2641–2643; e) I. M. Saez, J. W. Goodby, R. M. Richardson, *Chem. Eur. J.* **2001**, *7*, 2758–2764; f) S. A. Ponomarenko, E. A. Tatarinova, A. M. Muzafarov, S. Kirchmeyer, L. Brassat, A. Mourran, M. Moeller, S. Setayesh, D. de Leeuw, *Chem. Mater.* **2006**, *18*, 4101–4108.

[28] A. S. Matharu, S. J. Cowling, G. Wright, *Liq. Cryst.* **2007**, *34*, 489–506.

Received: September 3, 2009
Published online: October 28, 2010

